

## ON THE DISTANCE DETERMINATION AND IONIZATION OF THE HIGH-VELOCITY CLOUDS

A. FERRARA<sup>1,3,4</sup> AND G. B. FIELD<sup>2</sup>

Received 1993 May 3; accepted 1993 July 22

### ABSTRACT

We present a study of the ionization and thermal structure of neutral hydrogen clouds located in the Galactic halo, immersed in the extragalactic background radiation field, and supposed to be in pressure equilibrium with the surrounding (presumably) hot medium. The problem is solved numerically, but an useful analytical approximation has been derived as well. We discuss the two main parameters of the problem, i.e., the radiation field and the halo pressure, in the framework of the current models for the halo/disk interaction. We find a well defined relation between a critical column density at which the cloud starts to develop a cold central core with the cloud linear size. Making use of this relation, we suggest a straightforward method to derive the distance to the cloud. We discuss the possible sources of error in this determination and it is found that the method is particularly suitable for those clouds which are subsonic with respect to the surrounding medium, while for the supersonic ones, the method can only give a lower limit to the distance. The H $\alpha$  emission from the partially ionized edge of the cloud is calculated and compared with the available observations; this measure is a powerful indicator of the possible presence of a shock in the cloud.

*Subject headings:* Galaxy: halo — ISM: clouds — radio lines: ISM — shock waves

### 1. INTRODUCTION

One of the most long-standing problems in the study of the interstellar medium is represented by the so-called high-velocity clouds (HVCs). Generally speaking, HVCs were historically defined as clouds of neutral gas with a velocity relative to the LSR  $|v_{\text{LSR}}| \gtrsim 90 \text{ km s}^{-1}$ . Here we use the term in a somewhat looser manner, since we mean the H I cloud with velocities incompatible with a simple model of Galactic rotation and structure. The only requirement is that the clouds are located well above the main Galactic disk into the halo. The mass flux on the Galactic disk provided by the HVCs and the very high-velocity clouds (VHVCs), is about  $0.5 M_{\odot} \text{ yr}^{-1}$  (Mirabel 1989); Sembach, Savage, & Massa (1991) and Wakker (1991) derive a value of about  $5 M_{\odot} \text{ yr}^{-1}$  including all H I with velocities not fitting Galactic rotation. An estimate of their metallicity given by de Boer & Savage (1984) is  $Z \leq 0.3 Z_{\odot}$ ; similar results are obtained by Blades et al. (1988) for two HVCs in the direction of SN 1987A. HVCs are usually observed in H I 21 cm line emission; however in the last years a number of different observations have been attempted. Colgan, Salpeter, & Terzian (1990, and references therein) have reported a negative result in detecting the 21 cm absorption line, which they interpret as a requirement for an external heating source. Wakker & Boulanger (1986) have used the IRAS data to search for 100  $\mu\text{m}$  emission from dust inside the HVCs but none of the sample clouds has been detected. This implies a lower-than-normal dust content or a low temperature of the dust. There are no direct evidences of molecular hydrogen related to the HVC, even if Rohlfs et al. (1989) suggest that the high-latitude molecular cloud G90+38 can be spatially con-

nected with an infalling HVC. Absorption lines toward halo stars and extragalactic objects may provide useful information on the composition of the HVCs. However, the only firm detection of a HVC in a stellar spectrum is towards the star HD 135485 (Albert et al. 1989). Very recently, Bowen & Blades (1993) have detected for the first time Mg II absorption lines from two HVCs, which are part of the Complex C, in the line of sight of Mrk 205. Their results suggest a very different column density ratio  $N(\text{Mg II})/N(\text{H I})$  in the two clouds, which might be explained by a real difference in the metal content of the two clouds or by a difference in the ionization conditions: it is important to note at this regard, that the H I column densities for the two clouds differ roughly by a factor 10 (typical H I column densities for HVCs are in the range  $10^{18} < N_{\text{H}} < 10^{21} \text{ cm}^{-2}$ ). A relevant feature, discovered through the high-resolution synthesis maps (Wakker & Schwarz 1991), is the presence of bright, dense cores with  $N_{\text{H}}$  well in excess of  $10^{20} \text{ cm}^{-2}$ . A type of structure for the clouds made by bright concentrations with low-velocity widths ( $\sim 7 \text{ km s}^{-1}$ ) and extended envelopes with much larger widths ( $\sim 23 \text{ km s}^{-1}$ ) was already indicated by Cram & Giovanelli (1976).

As can be realized from the previous discussion, our understanding of the HVC phenomenon is quite fragmentary and incomplete. Definitely, the major source of ignorance is the lack of a precise distance estimate. The central importance of the distance knowledge has been stressed by many authors (van Woerden 1993, and references therein). From the observational point of view, the claim made by Danly, Albert, & Kuntz (1993) of the bracketing of the distance to a HVC in the Complex M in the range  $1.5 < z < 4.4 \text{ kpc}$ , provides at least the first firm evidence that the HVCs are located in the Galactic halo. The distance estimate is particularly important because most of the physical parameters of the clouds scale with the distance  $\Delta$ : the physical size,  $l \propto \Delta$ , the density,  $n \propto \Delta^{-1}$ , and the mass,  $M \propto \Delta^2$ . In addition the related problem of the origin of the HVCs could also strongly benefit from such an information. The most common explanation for the origin of the HVCs is the so-called Galactic fountain model

<sup>1</sup> Space Telescope Science Institute, 3700 San Martin Drive, Baltimore, MD 21218.

<sup>2</sup> Harvard-Smithsonian Center for Astrophysics, 60 Garden Street, Cambridge, MA 02138

<sup>3</sup> Osservatorio Astrofisico di Arcetri, Largo E. Fermi, 5, 50125 Florence, Italy.

<sup>4</sup> Affiliated with the Space Science Department, ESA.

(GF) worked out by Shapiro & Field (1976) and subsequently detailed by Bregman (1980); Houck & Bregman (1990) extended it to the low regions of the halo; Li & Ikeuchi (1992) have investigated their formation in giant halos. In this model the HVCs correspond to the condensation mode of a thermal instability occurring in a flow of hot gas, generated by supernova explosions, rising from the disk. Although the GF can explain most of the data concerning the HVCs (but not all: see the discussion in Wakker 1989), many doubts are still present on the reality of the entire circulation process. In fact, it is not completely clear that the superbubbles are able to breakout of the disk when the thick ("Lockman") exponential layer of the H I disk is considered (Mac Low & McCray 1988; Mac Low, McCray, & Norman 1989; Tenorio-Tagle, Rożyczka, & Bodenheimer 1990), and particularly when the effects of a magnetic field inhibiting the growth of the supernova shock-swept region are taken into account (Tomisaka 1990; Ferriere, Mac Low, & Zweibel 1991; Shapiro & Benjamin 1993; Norman 1993). On a different basis Ferrara & Einaudi (1992) pointed out that, under the regime prevailing in a fountain flow, dynamical instabilities, leading to convective motions rather than nongravitational condensations, may have a faster growth rate, thus quenching the cloud formation process. On the other hand, clear evidence of hot gas ( $T_h \gtrsim 10^6$  K) located in the Galactic halo comes from the *ROSAT* shadowing experiments toward the Draco cloud (Burrows & Mendenhall 1991; Snowden et al. 1991; Herbstmeier et al. 1993). Also, Herbstmeister et al. (1993) report an enhancement of the soft X-ray emission near some HVCs in the northern sky. This result brings fresh support to the existence of an extended hot halo and poses some constraints on its physical characteristics. It is probably redundant to stress at this point the value of the distance determination in order to make some progress on the origin of the HVCs: if they are located in the halo they must be in pressure equilibrium with the hot gas in order not to be rapidly dispersed; furthermore the study of this interaction may lead to a better comprehension of many different phenomena (accretion of material onto the Galactic disk, halo and disk star formation, Galactic chemical evolution, general gas circulation, structure of the halo) that are still unclear.

Finally, if HVCs are located well above the main gaseous Galactic disk, they are exposed to the ionizing extragalactic background radiation field (EBR). For the purpose of obtaining a determination of this field at redshift  $z = 0$ , the HVCs are an ideal "test particle," being a relatively quiet and little contaminated environment. This point have already been stated by other authors (Cowie & McKee 1976; Cowie & Songaila 1986; Songaila, Cowie, & Weaver 1988); in addition, the local value of the EBR has been recognized to be crucial in constraining many cosmological models. The principal response of the clouds to the ionizing radiation is the H $\alpha$  recombination emission. A number of searches of this emission have been performed in the last years: at least one positive detection has been reported (Kutyrev & Reynolds 1989).

In this paper we are proposing a new method to derive the distance to the HVCs based on a photoionization model for the clouds, supposed to be irradiated by the EBR. We will show that the observed core/envelope structure of many HVCs can be used to derive the cloud linear size, and, from the knowledge of the angular size, the distance to the cloud can, in principle, be obtained. Of course, there are possible sources of error in the method either of theoretical and observational nature, and we discuss the first ones and point out the possible

observational difficulties. Also, matching the H $\alpha$  emission deduced from the model to the observed one, further insight on the physical state of the cloud can be obtained.

The structure of the paper is as follows. In § 2 we describe the adopted photoionization model and discuss its relevant parameters; § 3 is dedicated to the results and to the distance estimation method, while in § 4 some additional implications are discussed.

## 2. IONIZATION MODEL

The equations governing the steady-state ionization and thermal balance of a cloud immersed in an isotropic radiation field of intensity  $I_\nu$  are

$$n(X^i) \int_{\nu_{LX}}^{\infty} \frac{J_\nu}{h\nu} \sigma_\nu(X^i) d\nu [1 + \phi(X^i)] + \gamma_c(X^i, T) n(X^i) n(e) = n(X^{i+1}) n(e) \alpha(X^i, T), \quad (2.1)$$

$$\sum_i \sum_X n(X^i) \int_{\nu_{LX}}^{\infty} \frac{J_\nu}{h\nu} h[\nu - \nu_{LX}] \sigma_\nu(X^i) d\nu = \sum_i \sum_X \mathcal{L}(X^i), \quad (2.2)$$

$$n(e) = \sum_i \sum_X i n(X^i), \quad i = 0 \dots, \quad (2.3)$$

$$P = kT \left[ n(e) + \sum_i \sum_X n(X^i) \right]. \quad (2.4)$$

These equations express the ionization and thermal balance, and charge conservation, while equation (4) is the equation of state for the gas;  $X$  denotes the element considered and  $i$  denotes its state of ionization;  $J_\nu$  is the first moment of the field,  $\nu_{LX}$  indicates the ionization limit for each species,  $\sigma$  is the photoionization cross section,  $\phi$  is the secondary ionization rate,  $\gamma_c$  is the collisional ionization coefficient,  $\mathcal{L}$  indicates the appropriate volume cooling rate, and  $\alpha$  is the total recombination coefficient. We have adopted the "on the spot" approximation in which the diffuse field photons are supposed to be absorbed close to the point where they have been generated.

The various elements are divided in "primary," which enter the ionization-thermal equilibrium equations (2.1)–(2.4) and "secondary" which do not. In the following, H and He are considered as primary, while other elements (C, N, O, Si, Fe) just contribute to the cooling function and to the electron density (C only). Secondary elements are considered to be completely ionized by the UV field below 13.6 eV; a metallicity  $Z = 0.25 Z_\odot$  and a helium abundance equal to 0.1 H as been assumed throughout the paper. Double ionization of He has been neglected, and He fractional ionization has been supposed equal to the H one,  $x$ ; the ionization cross section for He has been taken from Brown (1971). Helium is not of special importance in the temperature range that we consider; this justifies the rough approximation adopted. Secondary ionization rates and fractional heating for H and He have been taken from Shull & Van Steenberg (1985). The following processes have been included in the calculation of the cooling function: (i) free-free from all ions; (ii) H and He recombination; (iii) electron impact ionization of H and He; (iv) electron impact excitation of H and He ( $n = 2, 3, 4$  triplets); (v) He dielectronic recombination; (vi) electron and H impact excitation of secondary elements; excitation of the metastable levels by electron impact are also included. The obtained cooling function is almost identical to the one given by Dalgarno & McCray (1972). In addition to photoionization, heating is also provided

by C ionization (2 eV per ionization), assuming that the recombination coefficient  $\alpha$  for C is equal to the H one (Spitzer 1978). The numerical values for the various coefficients have been taken from Black (1981) and Dalgarno & McCray (1972).

In order to obtain the spatial ionization and thermal structure of the cloud, equations (2.1)–(2.4) must be solved simultaneously with the radiation transfer equation. We have postulated that the cloud can be modeled as a slab of gas of thickness  $l$  illuminated on both sides by the (isotropic) radiation field  $I_\nu$ . With the above assumption the transport equation reads

$$\frac{dI_\nu(z)}{dz} = -[n(\text{H})\sigma_\nu(\text{H}) + n(\text{He})\sigma_\nu(\text{He})]I_\nu(z), \quad (2.5)$$

which gives the solution

$$J_\nu(z) = 2\pi I_{\nu,0} \{E_2[t_\nu^+(z)] + E_2[t_\nu^-(z)]\}, \quad (2.6)$$

where  $E_2$  is the exponential integral function,  $I_{\nu,0}$  is the field intensity at the cloud edge, and

$$t_\nu^+(z) = \int_z^{l/2} [n(\text{H})\sigma_\nu(\text{H}) + n(\text{He})\sigma_\nu(\text{He})](1-x)dz \quad (2.7)$$

$$t_\nu^-(z) = \int_{-l/2}^z [n(\text{H})\sigma_\nu(\text{H}) + n(\text{He})\sigma_\nu(\text{He})](1-x)dz \quad (2.8)$$

The system of equations (2.1)–(2.5) can be numerically solved through an iterative scheme. We have requested the pressure  $P$  to be constant throughout the cloud; this condition is particularly suitable to describe the HVCs, which are believed to be in pressure equilibrium with a hot external medium. This argument, initially introduced by Spitzer (1956), is based on the fact that the pressure of the disk intercloud gas at 1 kpc would be far too low to confine the cloud, which would rapidly expand decreasing the density to values not allowing the detection of any spectral absorption feature toward distant stars.

In analogy with the usual H II regions, we expect to find a critical length,  $l_c$ , analogous to the usual Strömgren radius. The latter can be dimensionally evaluated equating the number of available ionizing photons to the number of recombinations inside a sphere, but in principle one can calculate the structure of the partially ionized zone at the interface between the cloud and the surrounding medium using some analytical approximations for eqs. (2.1)–(2.5). If we neglect secondary and collisional ionizations, the electron contribution due to secondary elements and helium, one can write the ionization equation in the isobaric case and for a power-law exciting spectrum of the form  $J_\nu = J_0(v/v_L)^{-\gamma}$  as

$$\frac{x^2}{(1-x)} = \frac{J_0 \int_{v_L}^{\infty} dv (\sigma_\nu/h\nu)(v_L/v)^\gamma}{n\alpha} = \frac{J_0 \zeta(1+x)kT}{P\alpha}, \quad (2.9)$$

where  $\zeta$  denotes the integral. In terms of the ionization parameter  $\Xi = P/J_0 \zeta$ , equation (2.9) becomes

$$\frac{x^2}{(1-x^2)} = \frac{kT}{\Xi\alpha}; \quad (2.10)$$

the transport equation (2.5) can also be simplified to give

$$\frac{dJ_0}{dz} = - \left[ \int_{v_L}^{\infty} dv \sigma_\nu (1-x)n \right] J_0 \simeq - \frac{1}{4} \sigma_{v_L} \frac{(1-x)}{(1+x)} \frac{P}{kT} J_0, \quad (2.11)$$

where  $\sigma_{v_L} = \sigma_\nu(v_{L,H})$ . Substituting for  $J_0$  and  $dJ_0/dz$  from equations (2.9)–(2.11) we obtain the equation for the spatial behavior of the ionization fraction:

$$\int_{x_0}^x \frac{dx}{(1-x)^2 x} = - \int_0^z dz \frac{\sigma_{v_L} P}{8kT}, \quad (2.12)$$

where  $x_0 = x(z=0)$  can be directly derived from equation (2.10):

$$x_0 = \sqrt{\frac{1}{1 + (\Xi\alpha/kT)}}. \quad (2.13)$$

Since both the integrand and the integral limits of equation (2.12) depend on the temperature, some additional approximation is required. To estimate the value of the temperature we run the numerical code for an optically thin case to calculate the (constant) value of the temperature  $T_0$  to be substituted in equation (2.13) as a function of  $\Xi$ . In addition, in order to integrate equation (2.12), we assume that the temperature inside the cloud remains approximately constant at the value  $T_0$ . Since most of the cooling mechanisms depend on the electron density  $n_e$ , this simplification is fairly good for a relatively high ( $x \gtrsim 0.70$ ) ionization fraction. In this case we find that the equation of state of the gas closely resembles a polytropic law

$$P \propto \rho^{(n/n+1)}, \quad n = -6.25; \quad (2.14)$$

the properties of polytropes with negative indexes have been studied by Viala & Horedt (1974). The solution  $x(z)$  of equation (2.13) is then implicitly given by

$$\log \frac{x}{|x-1|} - \frac{1}{(x-1)} = C_1 - \frac{z}{\lambda}, \quad (2.15)$$

where  $C_1 = \log x_0/|x_0-1| - (x_0-1)^{-1}$ ,  $\lambda = 8kT/\sigma_{v_L} P$ , and now  $x_0$  is calculated for  $T = T_0$  obtained numerically. Figure 1 shows various solutions of equation (2.15) for different values of the ionization parameter, for a spectral index  $\gamma = 1.4$ .

The main feature of the solutions is that, as one may expect,  $l_c$  tends to become smaller for large values of  $\Xi$  but the front is smoother. Also, for low values of  $\Xi$ , the ionized zone can be as

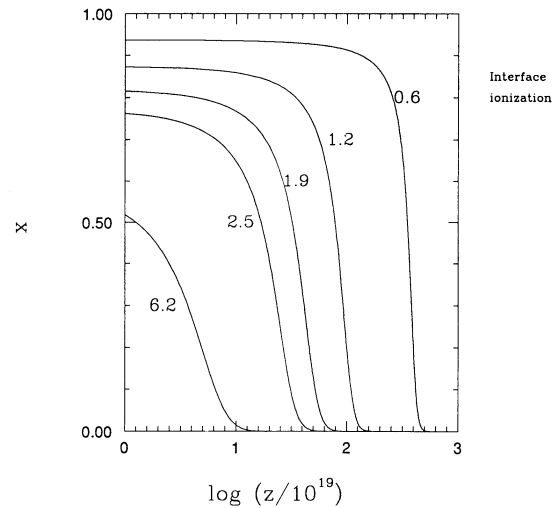


FIG. 1.—Ionization structure of the cloud partially ionized zone. The curves show the solutions of eq. (2.15); the numbers refer to different values of the ionization parameter  $\Xi = P/J_0 \zeta$ ;  $z$  is measured from the cloud edge.



deep as several kpc, and that means that in *low-pressure region HVCs are not expected to have a dense, cold core*. Although only approximate, the solutions found can be used to gain a qualitative insight of the problem and may serve as a test for the numerical scheme.

In the following we will discuss the two main input parameters of the problem, namely the radiation field and the pressure of the Galactic halo.

### 2.1. Halo Radiation Field

The ionizing radiation field in the halo is the sum of different components: the stellar radiation field from the disk, the quasar component and the X-ray background. As far as the disk contribution is concerned we will neglect it for the following reason. According to Brown & Gould (1970) (there is no appreciable difference at low energies with respect to the improved photoelectric cross sections given by Morrison & McCammon 1983) the energy at which half of the radiation is absorbed by gas in the Galactic disk is

$$\left(\frac{E^*}{\text{keV}}\right) = \left(\frac{N_{\text{H}}}{5.9 \times 10^{21} \text{ cm}^{-2}}\right)^{3/8}. \quad (2.16)$$

If we consider the value of  $N_{\text{H}} = 3.1 \times 10^{20} \text{ cm}^{-2}$  appropriate for the thick H I exponential distribution as given by Dickey & Lockman (1990), then  $E^* = 0.33 \text{ keV}$ . Thus, unless the H I is very clumpy (a claim that has no actual observational support, Jahoda et al. 1985), it seems very unlikely that any source of hard photons located in the stellar disk may contribute sensibly to the halo radiation field. Photons from a population of hot stars like the central stars of planetary nebulae and white dwarfs with a larger scale height could be able to penetrate the layer, but their number is quite uncertain. In addition, even if present in appreciable number, these photons are barely sufficient to maintain the ionization of the electron component that is known to extend out to about  $\sim 1.0 \text{ kpc}$  as pointed out by Reynolds (1990, 1993) and Nordgren, Cordes, & Terzian (1993). In this sense the electron component almost totally insulate the halo from the Galactic ionizing radiation. The same conclusion can be drawn if one considers photons escaping from the open chimneys (Norman & Ikeuchi 1989): again the majority of the photons are needed to maintain the ionization of the electron layer (Norman & Panagia 1991). Thus it appears that works including the contribution from photons escaping in the halo from the interior of multisupernova remnants (Bregman & Harrington 1986) are overestimating the ionizing flux.

A model for the radiation field in the halo proposed by Fransson & Chevalier (1985) has been widely used. The spectrum given by those authors is the sum of the quasar component obtained by Sargent et al. (1979) using the Schmidt luminosity distribution and the extragalactic X-ray background measured by Schwartz (1979). Lately, new studies have become available either theoretical and observational. While the X-ray portion of the spectrum given by Schwartz (1979) has been confirmed by recent observations by *Ginga* (for a review see McCammon & Saunders 1990), for what concerns the QSO radiation field the newly obtained quasar luminosity functions have produced different estimates of the QSO contribution to the local UV extragalactic background (Terasawa 1992; Madau 1992). Madau (1992) includes the effects of the opacity associated with the intervening Ly $\alpha$  clouds and Ly-limit absorption systems. Therefore, when these results are considered for the UV region of the EBR, we obtain the adopted

spectrum

$$I_{\nu}(E) = \begin{cases} 5.96 \times 10^{-24} E_{\text{Ry}}^{-1.4} & 13.6 \text{ eV} \leq E \leq 1.5 \text{ keV}; \\ 5.1 \times 10^{-26} E_{\text{keV}}^{-0.4} e^{-E/4.1 \text{ keV}} & 1.5 \text{ keV} \leq E \end{cases} \quad (2.17)$$

Note that this value is in agreement with the estimate  $I_{\nu}(\text{Ry}) \simeq 6 \times 10^{-24}$  derived by Kulkarni & Fall (1993) from a proximity effect study in the distribution of Ly $\alpha$  forest lines at low redshift.

To take into account the possible radiative contribution from the hot confining gas, we have also used a composite spectrum which is a sum of the EBR and the hot gas emission contributions. For a plasma temperature  $T_{\text{h}} \sim 10^6 \text{ K}$  the continuum emission is dominated by the free-free processes (Landini & Monsignori Fossi 1990). The intensity of the free-free emission can be written as

$$I_{\text{vff}}(E) = 1.66 \times 10^{-20} (\text{EM}) T_{\text{h}}^{-0.5} g(\nu, T_{\text{h}}) \sum \frac{Z^2 n_{\text{z}}}{n_{\text{H}}} e^{-E/kT_{\text{h}}}, \quad (2.18)$$

where EM is the emission measure,  $T_{\text{h}}$  is the temperature of the plasma,  $g(\nu, T_{\text{h}})$  is the Gaunt factor,  $Z$  is the ion charge, and  $n_{\text{z}}/n_{\text{H}}$  is its abundance; following Landini & Monsignori Fossi (1990), we have included only H and He. The adopted values for the hot gas are taken from Burrows & Mendenhall (1991) who have derived  $T_{\text{h}} = 1.25 \times 10^6 \text{ K}$  and  $\text{EM} = 0.006 \text{ cm}^{-6} \text{ pc}$ .

However, from an inspection of Figure 9 of Landini & Monsignori Fossi (1990), it appears that, at the  $T_{\text{h}}$  of interest, the total cooling losses are dominated by line emission, whose emissivity is about 18 times larger than the continuum one. In order to take into account this aspect, although in a rough manner, we assume that the spectral *shape* of the total emission from the hot gas (continuum + lines) is the same as the free-free but with a coefficient larger by a factor 18. This should be a reasonable assumption since the overwhelming majority of the lines for such a plasma are in the region shortward of 912 Å.

### 2.2. Halo Pressure

The determination of the pressure the Galactic halo is a difficult task because it involves a firm understanding not only of the disk/halo interaction, but also of the processes occurring at the interface with the intergalactic medium. A great deal of uncertainty, as already discussed in the introduction, persist on the nature (if any) of the disk/halo gas circulation. This topic has been recently reviewed by Spitzer (1990), who has also pointed out that the relationship among quiet phenomena as the buoyant gas in a fountain and highly dynamic transient ones is far to be clear. In addition, the question if the halo can be understood on average as a steady, and perhaps even static, structure still remains unanswered; nevertheless, many authors have investigated one-dimensional hydrostatic models for the halo (Fransson & Chevalier 1985; Hartquist & Morfill 1986; Bloemen 1987; Boulares & Cox 1990). The purpose of this section is to use some of these results together with simple estimations to obtain reasonable limits to the halo pressure.

#### 2.2.1. Dynamical Models

Recently, Li & Ikeuchi (1992), have investigated the formation of giant halos around spiral galaxies. Their paper provides useful information about the pressure distribution in dynamically, fountain-dominated halos. Among the three types of

halos they find (wind, bounded, and cooled) only the last one (cooled) forms HVCs by thermal instabilities in a region between  $0 \leq \varpi \leq 20$  kpc and  $0 \leq z \leq 10$  kpc, well out of the main galactic disk. The density and temperature vary quite rapidly in this region as can be realized from their Figures 8a and 8b and, therefore, rather than looking for a regular pattern we just derive an upper and lower limit to the pressure:

$$1.3 \times 10^{-17} \leq P \leq 2.3 \times 10^{-14} \text{ ergs cm}^{-3}; \quad (2.19)$$

all the intermediate values are present in the cloud forming layer. This halo corresponds to a temperature and density at the disk  $T_0 = 10^6$  K and  $n_0 = 5 \times 10^{-3} \text{ cm}^{-3}$ , therefore  $\log P_0/k = 3.7$ . It has to be pointed out that the pressure derived by Li and Ikeuchi is generally much lower than the one of the intergalactic medium (see next section), whose presence they did not consider. This could represent an inconsistency for their model.

### 2.2.2. Static Models

The static model can be ideally divided in “hot” and “cold” ones, i.e., in which the gas support comes from its own thermal pressure or from pressure contained in other phases (magnetic fields, cosmic rays, turbulent motions), respectively.

The simplest model for a hot halo is the isothermal one. The two-dimensional pressure distribution in such a model can be derived from the hydrodynamic in a straightforward manner. The static Bernoulli equation can be written as

$$c_s^2 \log \rho(\varpi, z) + \phi(\varpi, z) = \psi(\varpi), \quad (2.20)$$

where  $\phi$  is the Galactic gravitational potential. The quantity  $\varpi$  is the galactocentric radius and  $\psi$  is an integration constant with respect to  $z$  that can be obtained from a comparison with the  $\varpi$ -component of the steady momentum equation. For a constant galactic circular velocity  $v_\phi$ ,  $\psi(\varpi) = v_\phi^2 \log(\varpi) + C_2$ , where  $C_2$  is an integration constant. Therefore

$$P(\varpi, z) = P_\odot \left( \frac{\varpi}{\varpi_\odot} \right)^\beta e^{[\phi_\odot - \Phi(\varpi, z)]/c_s^2}, \quad (2.21)$$

where  $\beta = (v_\phi/c_s)^2$ . In order to avoid an unphysical result for  $\varpi \rightarrow \infty$  we must assume that far away  $\beta \rightarrow 0$ . This leads to the final expression,

$$P(\varpi, z) = P_\odot e^{[\Phi_\odot - \Phi(\varpi, z)]/c_s^2}. \quad (2.22)$$

When the limit

$$\lim_{z \rightarrow \infty} P(\varpi, z) = P_\odot e^{\Phi_\odot/c_s^2} = P_{\text{IG}},$$

where  $P_{\text{IG}}$  is the intergalactic pressure, is taken, given the values of  $P_{\text{IG}}$  and  $P_\odot$ ,  $c_s$  is uniquely determined. The value of the gravitational potential at the solar radius is  $\Phi_\odot = 4.8 \times 10^{14} \text{ cm}^2 \text{ s}^{-2}$  for a circular velocity  $v_\phi(\varpi_\odot) = 220 \text{ km s}^{-1}$  (Binney & Tremaine 1987). Assuming for the intergalactic medium  $T_{\text{IG}} = 10^8$  K and  $n_{\text{IG}} = 10^{-6} \text{ cm}^{-3}$ , and for  $P_\odot = 3.5 \times 10^{-12} \text{ ergs cm}^{-3}$  (Cox 1990), the derived temperature is  $T \sim 10^6$  K, exactly the same used as a boundary condition by the dynamical model of Li & Ikeuchi (1992). A plot of the pressure isocontour obtained from equation (2.22) is shown in Figure 2. The assumed potential is taken from de Boer (1991), also used by Ferrara (1993) to explain the vertical equilibrium of the Lockman component. It consists of an Oort vertical distribution and an exponential stellar radial potential:

$$\Phi(\varpi, z) = \sigma_g^2(\varpi) \left[ \log \cosh(z/z_0) + \frac{1}{2} \epsilon(\varpi)(z/z_0)^2 \right], \quad (2.23)$$

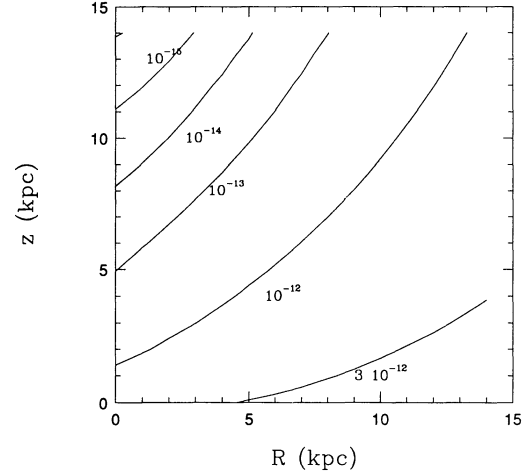


FIG. 2.—Pressure isocontours for a static, isothermal, hot halo; the temperature and pressure at the disk are  $T = 10^6$  K,  $P_\odot = 3.5 \times 10^{-12} \text{ ergs cm}^{-3}$ .

where  $z_0 = 250$  pc,  $\sigma_g^2(\varpi) = (15.4 \text{ km s}^{-1})^2 \exp(\varpi_\odot - \varpi)/0.44\varpi_\odot$ , and  $\epsilon = 0.04, 0.07, 0.14$  for  $\varpi = 5, 10, 15$  kpc, respectively. A quadratic interpolation to  $\epsilon$  has been used whenever required. In the region of interest ( $0 \leq \varpi \leq 20$  kpc,  $0 \leq z \leq 10$  kpc) the lower and upper limits for a hot static model from Figure 2 are

$$10^{-15} \leq P \leq 10^{-12} \text{ ergs cm}^{-3} \quad (2.24)$$

In the cold halo of models the support in the gravitational field is provided by sources different from thermal energy, as discussed above. We will refer, as a prototype, to the one-dimensional model presented by Boulares & Cox (1990), which appears to include the most updated data compilation of the distribution of the various phases of the ISM. A fit of the exponential component (which is the important one at high  $z$ ) of the pressure from their results gives the following expression for the solar neighborhood:

$$P(z) = 2.61 \times 10^{-12} e^{-z/1.23 \text{ kpc}} \text{ ergs cm}^{-3}. \quad (2.25)$$

In this region the lower and upper limits for the Boulares and Cox cold static model from equation (2.25) are

$$2.2 \times 10^{-13} \leq P \leq 7.7 \times 10^{-16} \text{ ergs cm}^{-3}. \quad (2.26)$$

The range of pressures obtained for the three different (dynamical, static hot/cold) types of halos is large and hence pretty unsatisfactory. This fact reflects the extremely poor comprehension of the halo and strongly recommends further theoretical and observational studies.

### 3. RESULTS AND THE DISTANCE METHOD

The method we are proposing in order to determine the distance to the HVCs is essentially based on their detailed ionization structure, which is completely determined by the five coupled equations (2.1)–(2.5). For this purpose we have solved those equations numerically for each point inside the cloud, supposed to have a slab geometry and subjected to an external fixed pressure  $P$ . Figures 3–5 show some of the results obtained for different values of  $P$ . The radiation field, illuminating the cloud from both sides, has been held fixed at this stage to the fiducial value given by equation (2.17), and this particular choice will be referred as the *standard* field. The two panels of each figure show the density and temperature profiles

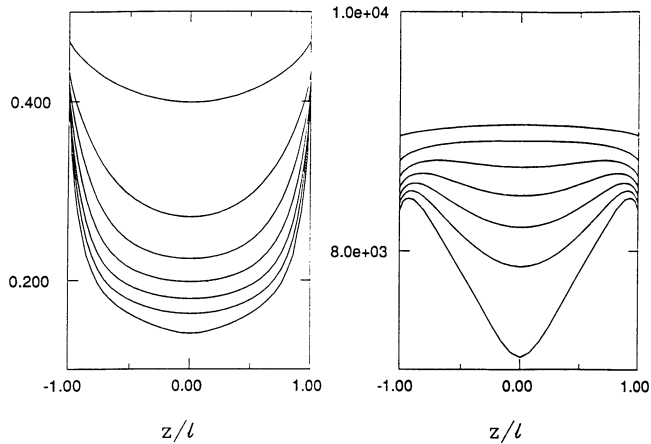


FIG. 3.—Ionization (right) and temperature (left) structure for a cloud of size  $l$  exposed to the standard EBR field given by eq. (2.17); the pressure is constant at a value  $P = 10^{-3}$  ergs  $\text{cm}^{-3}$ . Each line refers to a different value of the column density  $N_H$  which is in the range  $3 \times 10^{16} \leq N_H \leq 7.5 \times 10^{-7} \text{ cm}^{-2}$ .

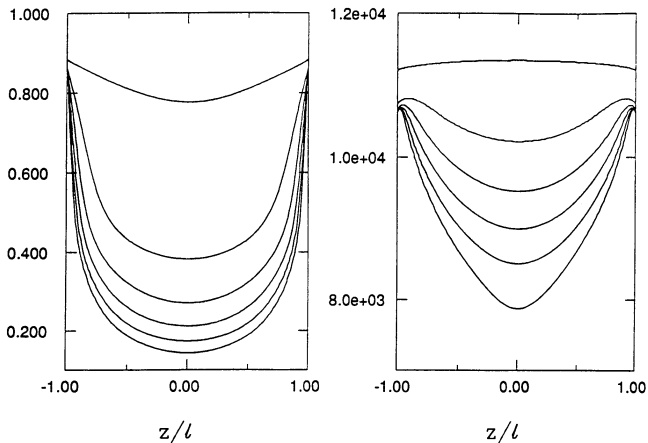


FIG. 4.—Same as Fig. 3, but for  $P = 10^{-14}$  ergs  $\text{cm}^{-3}$ , and  $5 \times 10^{16} \leq N_H \leq 8.5 \times 10^{18} \text{ cm}^{-2}$ .

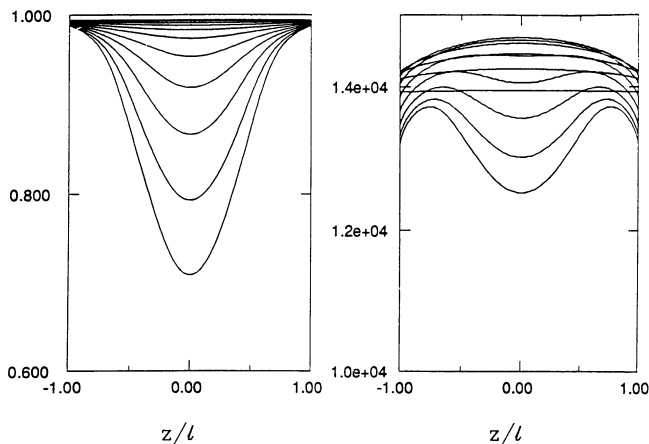


FIG. 5.—Same as Fig. 3, but for  $P = 10^{-15}$  ergs  $\text{cm}^{-3}$ , and  $1 \times 10^{15} \leq N_H \leq 1.4 \times 10^{18} \text{ cm}^{-2}$ .

as a function of the ratio  $z/l$ , where  $z$  is the depth inside the cloud and  $l$  is the cloud size. Note that different curves refer to different values of the H I column density and, therefore, of  $l$ ; obviously, solutions are symmetric about the point  $z/l = 0$  given that the symmetry properties of the problem.

As can be realized at a first glance to Figures 3–5, the ionization structure of the cloud strongly depends on the pressure of the external medium. Following the discussion in § 2.2, we have selected three different values of the pressure  $P$  that presumably may well represent the actual values, namely  $P = 10^{-15}$ ,  $10^{-14}$ ,  $10^{-13}$  ergs  $\text{cm}^{-3}$ . We have disregarded the value  $P = 10^{-12}$  ergs  $\text{cm}^{-3}$  because such a high pressure arises only in the static hot halo model and in regions close to the disk, where the contamination due to the galactic radiation field and local gaseous phenomena as outflows can become dominant. For  $P = 10^{-13}$  ergs  $\text{cm}^{-3}$ , the cloud is initially almost optically thin ( $l = 0.6$  pc,  $N_H = 2 \times 10^{16} \text{ cm}^{-2}$ ) with an ionization fraction  $x \sim 0.42$  and a temperature  $T \sim 9000$  K. When the size is increased, self-shielding effects become more and more important, especially in the central parts of the cloud, and the ionization and the temperature decrease steadily due to the decreased number of ionizing photons available. The temperature structure will develop a maximum not located at the cloud edge, but slightly displaced in the interior; this is due to the fact that close to the edge, the temperature is determined by the larger availability of electrons for cooling rather than by a decrease in the number of ionizing photons. Eventually (last two curves), the temperature starts to fall down in an abrupt manner, while the ionization preserves its regular pattern. Continuing to increase  $N_H$ , the cloud develops a cold core, due to photon exhaustion in the partially ionized zone. This fact confirms our simple analytical estimates of § 2, shown in Figure 1. The characteristics of this central dense ( $n \sim 40 \text{ cm}^{-3}$ ), cold ( $T \sim 20$  K) core are not directly relevant to the aim of this paper (anyway, some discussion is given below). The important point is, however, the existence of a critical column density  $N_H^c$ , corresponding approximately to the curves with the lowest ionization fraction shown in each figure, after which a central condensation completely shielded from the external radiation field is formed; in this case  $N_H^c \sim 7 \times 10^{17} \text{ cm}^{-2}$ . We will exploit this fact, as explained below, to determine the distance to the HVCs.

The same kind of behavior shown by the solutions for  $P = 10^{-13}$  ergs  $\text{cm}^{-3}$ , can be qualitatively recognized for the two other pressure values adopted. For  $P = 10^{-14}$  ergs  $\text{cm}^{-3}$  the ionization fraction is higher, particularly when the medium is still optically thin ( $x \sim 0.8$ ), and  $N_H^c \sim 10^{19} \text{ cm}^{-2}$ . Finally, when the pressure is set to  $P = 10^{-15}$  ergs  $\text{cm}^{-3}$ , the medium is almost completely ionized and in order to reach the critical column density the cloud size must be implausibly large ( $l \gtrsim 30$  kpc) if compared with any realistic model of the HVCs.

The previous results can be summarized in a  $N_H - l$  plane as the one presented in Figure 6. Each series of points represents the  $N_H - l$  relation for the curves previously discussed. According to the previous discussion, the plane can be divided in two subregions (Fig. 6): a lower one, in which the ionization front is “matter bounded” and clouds do not have any cold core, and an upper one in which the front is “radiation bounded” and a central cold core is found. Clouds located in the upper part of the plane have thus a composite structure made up by a neutral core surrounded by a warm envelope which constitutes an interface with the external, presumably hot, medium. A simple approximate expression for the



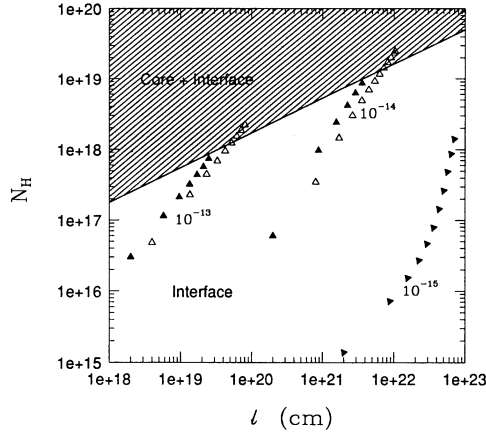


FIG. 6.—Hydrogen column density of the cloud as a function of its size; the numbers refer to different values of the pressure in ergs cm<sup>-3</sup>. Solid triangles refer to the standard EBR field given by eq. (2.17), open triangles are for the composite field EBR + free-free from hot gas. The upper dashed part describes the region of the parameter space in which the clouds develop a core + interface structure in the EBR field.

“critical” curve  $N_H^c(l)$  is found to satisfy

$$N_H^c(l) = N_1 \sqrt{l_{pc}} \text{ cm}^{-2}, \quad (3.1)$$

with  $N_1 = 3 \times 10^{17} \text{ cm}^{-2}$ . An analogous relation, which is a very good approximation in the range  $5 \times 10^{15} \lesssim P \lesssim 10^{-13} \text{ ergs cm}^{-3}$ , between  $N_H^c$  and  $P$  is

$$N_H^c(l) = N_2 P^{-1/13} \text{ cm}^{-2}, \quad (3.2)$$

where  $N_2 = 7.4 \times 10^{17}$  and  $P_{-13} = P/10^{-13}$ . In addition to the case in which only the EBR field is considered, the analogous results for the sum of the EBR + free-free ionizing spectrum is also reported in Figure 6. This addition is not modifying the results in a substantial way because of the relatively low EM of the hot gas, and hence of the low intensity of its radiation field. Note that there are no open triangles in the case  $P = 10^{-15} \text{ ergs cm}^{-3}$  because they are physically meaningless, indicating cloud sizes of the order of  $10^2 \text{ kpc}$ , larger than the halo itself; one may wonder about the extragalactic nature of HVCs (which is excluded by almost any sort of data), but the hypothesis of this paper should then be radically modified.

It is natural to identify the core + interface structure found with the observational evidences reported by many authors and discussed in the introduction, even if not much significance should be attached to the precise values of the line widths since nonthermal mechanisms may concur to the line broadening; the important point is the observed values, typically  $\gtrsim 20 \text{ km s}^{-1}$ , are higher than the ones corresponding to our solutions. At this point the suggested strategy to determine the distance to the HVCs becomes almost self-explanatory. In order to be as clear as possible we put it in a schematic form:

1. Using a cloud with a core + interface structure, measure its  $N_H$  in the interface; the measured  $N_H$  will hence correspond to the critical column density  $N_H^c$ .
2. The value of  $N_H^c$  must be located on the critical curve (3.1). This gives the linear size of the interface, which, given the existence of the core, must be exactly the  $l$  corresponding to that critical column density. By the way, pressure can be therefore immediately determined through relation (3.2).
3. Once the linear size of the interface  $l$  is known, from its angular diameter  $\theta$ , the distance  $\Delta$  can be found through the relation  $\Delta = l/2\theta$ .

The procedure is quite straightforward if the cloud is observed to have the required core + interface structure and column density measures are available. Note that the actual characteristics and column density of the core are not relevant to the distance determination. The mere existence of the core bounds the column density of the partially ionized zone (interface) to the appropriate critical density for the given pressure. Some inferences on the physical state of the cores can nevertheless be made. The very low temperature characterizing the cores in our model is to a large extent determined by the only heating mechanism included apart from the radiative one, i.e., C ionization. Other heating mechanisms can of course be foreseen; however, the nondetection of any HVCs in the *IRAS* maps (Wakker & Boulanger 1986), if interpreted as a low temperature of the dust, favors the idea that HVCs are a cool environment. However, the nondetection can be alternatively explained as due to a low dust abundance, since dust can be heavily sputtered during the expulsion process from the disk (Ferrara et al. 1991).

Adding another step to our procedure, we can also infer an approximate temperature of the core:

4. Using the measured core  $N_H$ , from the determination of its linear size  $l_c$  which is possible knowing  $\Delta$ , we obtain an average value of the density in the core  $\langle n_c \rangle$ , from which  $T_c$  can be derived from the equation of state.

From a theoretical point of view, there are two main mechanisms which can introduce some error in the distance determined according to the scheme presented. The first one is thermal conduction (Cowie & McKee 1976; Draine & Giuliani 1984; McKee & Begelman 1990; Ferrara & Shchekinov 1993) whose main effect is to broaden the ionized zone. However, if clouds are formed from a thermal instability in the fountain, by definition their size must be larger than the critical wavelength at which thermal instabilities become stabilized by conduction (Field 1965). Ferrara & Shchekinov (1993) have demonstrated that the dynamical effects of thermal conduction in such conditions are negligible. Also conductive interfaces at the steady state tend to have a remarkably flat temperature profile: for a spherical cloud,  $T(r) = T_h(1 - l/r)^{2/5}$ , where  $r$  is the distance from the cloud center and  $r \geq l$ , and thus most of the interface is at a temperature close to the one of the hot medium  $T_h$ . In these conditions virtually all the hydrogen is completely ionized and the contribution of this gas to  $N_H$  is negligible. A second mechanism providing ionization is mechanical input by shocks. The sound speed in the hot gas is

$$c_s = \left( \frac{\gamma P}{\mu m_p n_h} \right)^{1/2} = 126 \left( \frac{P_{-13}}{n_{-3}} \right)^{1/2} \text{ km s}^{-1}, \quad (3.3)$$

where it has been assumed that the mean molecular weight  $\mu = 0.65$ ,  $m_p$  is the proton mass, and  $n_{-3} = n_h/10^{-3}$  is the hot gas density; thus, by definition, some HVCs move subsonically for the reference values of equation (3.3). The emission measure integrated on a path of  $10 \text{ kpc}$  for such a hot gas is  $E_m(n_{-3} = 1) = 10^{-2} \text{ cm}^{-6} \text{ pc}$ , consistent with the one derived by the *ROSAT* soft X-ray shadowing experiments (Burrows & Mendenhall 1991; Snowden et al. 1991); also the temperature derived by a fit to the data is consistent with the estimate (3.3). Therefore, it appears that a relevant fraction of the HVCs should not be affected by a shock, unless a large transversal velocity component is present. However, shocks may have some importance in the thermal balance of the core, and eventually may lead to episodes of star formation, according to the

calculations made by Dyson & Hartquist (1983). Viscous heating,  $\mathcal{H} \propto \rho_h v^3$  is not going to be important given the low density of the hot medium. We conclude that the error on the distance determination due to the effect of thermal conduction is negligible; in addition, for those HVCs with velocity lower than  $c_s$  specified by equation (3.3), shocks are not expected to appear.

Probably more important are the possible errors related to real data. It could be difficult to locate observationally the position of the inner and outer edges of the interface in an accurate manner. The inner edge is defined as the limit of the region with narrow line profiles; however, this edge is often not regular. For the outer edge, instead, it is crucial to resort to high sensitivity data to detect the low H I column density associated with the external regions of the interface. In addition, our assumption of a slab geometry can introduce some additional error, particularly when the interface has dimensions much larger than the core. This could be avoided by appropriately selecting the cloud sample. With respect to the last point, we mention that in the framework of the fountain model, HVCs are predicted to have a sheetlike shape (Kahn 1991) which would make the slab geometry very appropriate.

From the previous discussion it appears that the direct application of the proposed method requires particular attention to both sample selection and the estimation of possible errors. We plan to present these results in a forthcoming publication; we stress, however, that a dedicated observational study could serve this purpose much better.

#### 4. FURTHER IMPLICATIONS

In the previous section we have presented a simple method based on the photoionization structure of the HVCs which can be used in order to obtain reliable distances to the clouds possessing a two-phase structure composed by a warm ionized interface and a cold neutral core. However, our treatment provides an opportunity to have some insight on some global properties of the Galactic halo and the EBR. This is possible if we compare the H $\alpha$  emission as predicted by our models with the one detected by Kutryev & Reynolds (1989, hereafter KR) and Songaila, Bryant, & Cowie (1989, hereafter SBC). The first authors report the detection of H $\alpha$  emission from a HVC situated in Cetus with a surface brightness  $I_\alpha = 8.1 \pm 1.9 \times 10^{-2}$  R (where one rayleigh corresponds to  $10^6/4\pi$  photons  $\text{cm}^{-2} \text{s}^{-1} \text{sr}^{-1}$ ); Songaila et al. deduce instead  $I_\alpha = 3 \times 10^{-2}$  R from two points in a HVC belonging to the Complex C. These are the only detections we are aware of and therefore, given the restricted sample, no definite conclusions can be drawn; the comparison could be anyway of some interest.

Assuming Case B recombination, the H $\alpha$  intensity integrated on our model slab cloud can be written as

$$I_\alpha = K \int_0^1 n^2 x (x + h_c + x h_{\text{He}}) T^{-0.96} dz \text{ R}, \quad (4.1)$$

where  $K = 8.17 \times 10^{-16}$ ,  $n$  is the total gas density,  $x$  is the fractional ionization and  $h_c$ ,  $h_{\text{He}}$  are the abundances of C and He relative to H, respectively. The results obtained applying equation (4.1) to the three models for low-, intermediate-, and high-pressure cases discussed in the previous section are shown in Figure 7 along with the observational results. It is immediately realized that the observed H $\alpha$  intensity is larger than the theoretical one for all the pressure cases considered and the discrepancy becomes larger as the pressure of the external

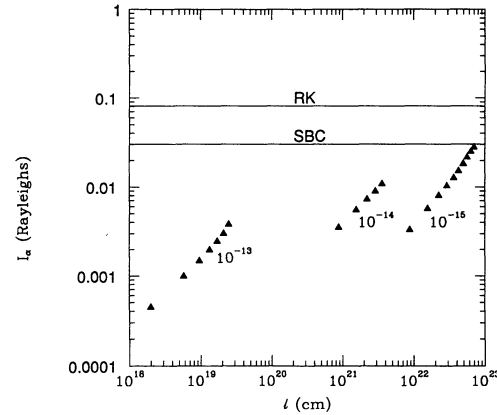


FIG. 7.—Calculated H $\alpha$  intensity,  $I_\alpha$ , from the cloud interface as a function of cloud size for the three models of Fig. 6; the numbers refer to different values of the pressure in  $\text{ergs cm}^{-3}$ . Also shown (horizontal lines) are the observed values for two HVCs as given by RK and SBC.

medium is increased. The explanations for this dicotomy can all be found in two basic possibilities, namely (i) the intensity of the radiation field must be larger than the one assumed, and/or (ii) some mechanical energy input must take place. As for the first point, it is difficult to conceive a dramatically different value from the EBR intensity given by equation (2.17): in fact, it has been proven able to explain several effects at high redshift and confirmed by observations in its high-energy part. If we exclude that any ionizing photon from the galaxy can escape the thick Reynolds layer, the only remaining source of ionizing photons may come from free-free emission of the hot gas confining the cloud. In the previous section we have seen that some modification to the ionization structure of the cloud and to the interface size can be introduced by the consideration of this contribution. However, the H $\alpha$  emission calculated from the models including the radiation field from the local hot gas show an enhancement only of a few percent with respect to the pure EBR field case and certainly not sufficient to explain the observed excess.

Thus we are left with the second possibility, i.e., H $\alpha$  emission is provided by recombinations following a shock wave created by the HVC/hot gas interaction. Support for this hypothesis comes from the two following evidences. First, the two clouds have velocities well in excess of the sound speed in the hot medium (eq. [3.3]): for the KR cloud  $|v_{\text{LRS}}| \sim 300 \text{ km s}^{-1}$ , while for the SBC one  $|v_{\text{LRS}}| \sim 140 \text{ km s}^{-1}$ ; second, the H $\alpha$  emission excess is correlated with the velocity as one would expect if part of the ionization is produced by a shock. We conclude that the suggested method is not applicable to those clouds in a straightforward manner since we have assumed that the ionization of the clouds is due to the radiation field (EBR + free-free) only; at any rate the distance method in such cases will provide at least a lower limit to the distance. This could be particularly useful if absorption features toward a background star are detected from the cloud. Finally, the calculated H $\alpha$  emission (Fig. 7) provides a powerful test of the conditions in which the proposed distance method can give reliable results, and clearly indicates the possible presence of a shock.

We thank S. M. Fall and an anonymous referee for useful comments.



## REFERENCES

- Albert, C. E., Blades, J. C., Morton, D. C., Proulx, M., & Lockman, F. J. 1989, in *Structure and Dynamics of the Interstellar Medium*, ed. G. Tenorio-Tagle, M. Moles, & J. Melnick (Berlin: Springer), 442
- Binney, J., & Tremaine, S. 1987, *Galactic Dynamics* (Princeton: Princeton Univ. Press)
- Black, J. H. 1981, *MNRAS*, 197, 555
- Blades, J. C., Wheatley, J. M., Panagia, N., Grewing, M., Pettini, M., & Wamsteker, W. 1988, *ApJ*, 332, L75
- Bloemen, J. B. G. M. 1987, *ApJ*, 322, 694
- Boulares, A., & Cox, D. P. 1990, *ApJ*, 365, 544
- Bowen, D. V., & Blades, J. C. 1993, preprint
- Bregman, J. N. 1980, *ApJ*, 236, 577
- Bregman, J. N., & Harrington, J. P. 1986, *ApJ*, 309, 833
- Brown, R. L. 1971, *ApJ*, 164, 387
- Brown, R. L., & Gould, R. J. 1970, *Phys. Rev. D.*, 1, 2252
- Burrows, D. N., & Mendenhall, J. A. 1991, *Nature*, 351, 629
- Colgan, S. W. J., Salpeter, E. E., & Terzian, Y. 1990, *ApJ*, 351, 503
- Cox, D. P. 1990, in *The Interstellar Medium in Galaxies*, ed. H. A. Thoronson & J. M. Shull (Dordrecht: Kluwer), 181
- . 1993, in *ESO/EIPC Workshop on Starburst Galaxies and Their Interstellar Medium*, ed. J. Franco & F. Ferrini (Cambridge: Cambridge Univ. Press), in press
- Cowie, L. L., & McKee, C. F. 1976, *ApJ*, 209, L105
- . 1977, *ApJ*, 211, 135
- Cowie, L. L., & Songaila, A. 1986, *ARA&A*, 24, 499
- Cram, T. R., & Giovanelli, R. 1976, *A&A*, 48, 39
- Dalgarno, A., & McCray, R. 1972, *ARA&A*, 10, 375
- Danly, L., Albert, C. E., & Kuntz, 1993, in *3d Annual Maryland Meeting, Back to The Galaxy*, (Washington: NASA), in press
- de Boer, H. 1991, in *The Interstellar Disk-Halo Connection in Galaxies*, ed. H. Bloemen (Dordrecht: Kluwer), 333
- de Boer, K. S., & Savage, B. D. 1984, *ApJ*, 136, L7
- Dickey, J. M., & Lockman, F. J. 1990, *ARA&A*, 28, 215
- Draine, B. T., & Giuliani, J. L. 1984, *ApJ*, 281, 690
- Dyson, J. E., & Hartquist, T. W. 1983, *MNRAS*, 203, 1233
- Ferrara, A. 1993, *ApJ*, 407, 157
- Ferrara, A., & Einaudi, G. 1992, *ApJ*, 395, 475
- Ferrara, A., Ferrini, F., Franco, J., & Barsella, B. 1991, *ApJ*, 381, 137
- Ferrara, A., & Shchekinov, Yu. 1993, *ApJ*, 418, in press
- Field, G. B. 1965, *ApJ*, 142, 531
- Ferriere, K., Mac Low, M. M., & Zweibel, E. G. 1991, 375, 239
- Herbstmeier, U., Kerp, J., Snowden, S. L., & Mebold, U. 1993, in *Star-Forming Galaxies and Their Interstellar Medium*, ed. J. Franco & F. Ferrini (Cambridge: Cambridge Univ. Press), in press
- Fransson, C., & Chevalier, R. A. 1985, *ApJ*, 296, 35
- Hartquist, T. W., & Morfill, G. E. 1986, *ApJ*, 311, 518
- Houck, J. C., & Bregman, J. N. 1990, *ApJ*, 352, 506
- Jahoda, K., McCammon, D., Dickey, J. M., & Lockman, F. J. 1985, *ApJ*, 290, 229
- Kahn, F. D. 1991, in *The Interstellar Disk-Halo Connection in Galaxies*, ed. H. Bloemen (Dordrecht: Kluwer), 1
- Kulkarni, V. P., & Fall, S. M. 1993, *ApJ*, 413, L63
- Kutyrev, A. S., & Reynolds, R. J. 1989, *ApJ*, 344, L9 (KR)
- Landini, M., & Monsignori Fossi, B. C. 1990, *AASS*, 82, 229
- Li, F., & Ikeuchi, S. 1992, 390, 405
- Mac Low, M. M., & McCray, R. 1988, *ApJ*, 324, 776
- Mac Low, M. M., McCray, R., & Norman, M. L. 1989, *ApJ*, 337, 141
- McKee, C. F., & Begelman, M. C. 1990, *ApJ*, 358, 392
- Madau, P. 1992, *ApJ*, 389, L1
- McCammon, D., & Sanders, W. T. 1990, *ARA&A*, 28, 657
- Mirabel, I. F. 1989, in *Structure and Dynamics of the Interstellar Medium*, ed. G. Tenorio-Tagle, M. Moles, & J. Melnick (Berlin: Springer), 396
- Morrison, R., & McCammon, D. 1983, *ApJ*, 270, 119
- Nordgren, T. E., Cordes, J. M., & Terzian, Y. 1993, preprint
- Norman, M. L. 1993, in *3d Annual Maryland Meeting, Back to The Galaxy* (Washington: NASA), in press
- Norman, C. A., & Ikeuchi, S. 1989, *ApJ*, 345, 372
- Norman, C. A., & Panagia, N. 1991, in *The Interstellar Disk-Halo Connection in Galaxies*, ed. H. Bloemen (Dordrecht: Kluwer), 325
- Reynolds, R. J. 1990, *ApJ*, 349, L17
- . 1993, in *3d Annual Maryland Meeting, Back to The Galaxy* (Washington: NASA), in press
- Rohls, R., Herbstmeier, U., Mebold, U., & Winnberg, A. 1989, *A&A*, 211, 402
- Sargent, W. L. W., Young, P. J., Boksenberg, A., Carswell, R. F., & Whelan, J. A. J. 1979, *ApJ*, 230, 49
- Schwartz, D. A. 1979, in *X-Ray Astronomy*, ed. W. A. Baity & L. E. Peterson (Oxford: Pergamon), 453
- Sembach, K. R., Savage, B. D., & Massa, D. 1991, *ApJ*, 372, 81
- Shapiro, P. R., & Benjamin, R. A. 1993, in *Star-Forming Galaxies and Their Interstellar Medium*, ed. J. Franco & F. Ferrini (Cambridge: Cambridge Univ. Press), in press
- Shapiro, P. R., & Field, G. B. 1976, *ApJ*, 205, 762
- Shull, J. M., & Van Steenberg, M. E. 1985, *ApJ*, 298, 268
- Snowden, S. L., Mebold, U., Hirth, W., Herbstmeier, U., & Schmitt, H. M. M. 1991, *Science*, 292, 1529
- Songaila, A., Bryant, W., & Cowie, L. L. 1989, *ApJ*, 345, L71 (SBC)
- Songaila, A., Cowie, L. L., & Weaver, H. 1988, *ApJ*, 329, 580
- Spitzer, L. 1956, *ApJ*, 124, 20
- . 1978, *Physical Processes in the Interstellar Medium* (New York: Wiley)
- . 1990, *ARA&A*, 28, 71
- Tenorio-Tagle, G., Rożyczka, M., & Bodenheimer, P. 1990, *A&A*, 237, 207
- Terasawa, N. 1992, *ApJ*, 392, L15
- Tomisaka, K. 1990, *ApJ*, 361, L5
- van Woerden, H. 1993, in *Luminous High-Latitude Stars*, ed. D. D. Sasselov (ASP Conf. Ser.), in press
- Viala, Y. P., & Horedt, G. 1974, *A&A*, 33, 195
- Wakker, B. P. 1989, Ph.D. thesis, Groningen Univ.
- . 1991, in *The Interstellar Disk-Halo Connection in Galaxies*, ed. H. Bloemen (Dordrecht: Kluwer), 27
- Wakker, B. P., & Boulanger, F. 1986, *A&A*, 170, 84
- Wakker, B. P., & Schwarz, U. J. 1991, *A&A*, 250, 484